Pergamon

J. Aerosol Sci. Vol. 30, No. 8, pp. 1019–1028, 1999

Printed in Great Britain

PII: S0021-8502(98)00789-7

0021-8502/99/$ - see front matter

PARTICLE TRANSMISSION EFFICIENCY THROUGH THE NOZZLE OF THE API AEROSIZER™

Chuen-Jinn Tsai,*† Wu-Song Yang,† Wladyslaw W. Szymanski‡ and Hung-Min Chein§

† Institute of Environmental Engineering, National Chiao Tung University, No. 75 Poai St., Hsin Chu, Taiwan
‡ Institute of Experimental Physics, University of Vienna, Boltzmanngasse 5, A-1090, Vienna, Austria
§ Center for Industrial Safety and Health Technology, Industrial Technology Research Institute, Hsin Chu, Taiwan

(*First received* 30 *May* 1998; *and in final form* 1 *December* 1998)

Abstract—This study has investigated the particle transmission efficiency through the nozzle of the API Aerosizer™ numerically. Two-dimensional flow field in the nozzle was first simulated. Particle trajectories for both liquid and solid particles were then calculated to obtain the particle transmission efficiency under various conditions. This study shows that particle aerodynamic diameter, particle materials, particle density and laser beam diameter influence the transmission efficiency. The transmission efficiency is found to increase with increasing particle diameter when the particle aerodynamic diameter is less than several micrometers. The efficiency for liquid particles drops significantly when particle aerodynamic diameter increases from several micrometers because of particle impaction loss in the nozzle. For solid particles, the relationship of the efficiency with particle diameter is found to be more complicated. For particles less than several micrometers in aerodynamic diameter, solid particles behave similarly to the liquid particles. However, as particles are greater than several micrometers, the effect of solid particle bounce is to increase the transmission efficiency with increasing aerodynamic diameter until particles become large enough so that plastic deformation occurs in the particles. Then the transmission efficiency will decrease with increasing particle aerodynamic diameter.

INTRODUCTION

The API Aerosizer™ (Amherst Process Instruments Inc., Amherst, MA, USA) is an aerosol spectrometer used to measure size distributions of airborne particles in real time. Its design is based on the research of Dahneke (1973), Dahneke and Padliya (1977), Dahneke and Cheng (1979), and Cheng and Dahneke (1979). The Aerosizer is claimed to be capable of measuring particles of diameters between 0.2 and 700 μm, determining up to 10,000 particles per second with 5% accuracy, and discriminating between two particles differing in diameter by less than 10% (API, Inc., 1992). Its claimed wide range of measurement in real time surpasses other aerosol instruments and the instrument has been used in many aerosol measurement applications (Terzieva *et al*., 1996; Bohan, 1996; Etzler and Deanne, 1997; de Juan and Fernandez de la Mora, 1997; Ulevicius *et al*., 1997; Grinshpun *et al*., 1997).

However, some limitations and problems of API Aerosizer have been found recently by researchers. Comparison of the Aerosizer with other aerosol measurement devices shows that this instrument is not suitable for airborne particles of diameter below 0.5 μm at normal atmospheric pressure (Grinshpun *et al*., 1995; Qian *et al*., 1995). The Aerosizer significantly underestimates aerosol concentrations and affects the accuracy of aerodynamic particle size at reduced pressures (Cheng *et al*., 1993; Grinshpun *et al*., 1997). The instrument's response depends on ambient conditions and calibration is suggested at different ambient pressure other than standard atmospheric pressure (Cheng *et al*., 1993). Theoretical time-of-flights of particles calculated from one dimensional flow field and incorrect drag coefficients underestimate the experimental data (Tsai *et al*., 1998). Particle density and dynamic shape factor influence sizing accuracy of aerosols (Marshall and Mitchell, 1992; Cheng *et al*., 1993; Tsai *et al*., 1998). Particle diameter, particle

* Author to whom correspondence should be addressed.

concentration, photomultiplier tube (PMT) voltage, and model type also influence Aerosizer's counting accuracy (Mitchell and Nagel, 1996; Thornburg *et al*., 1999). For liquid oleic acid particles less than 8 μm in diameter, the counting efficiency was shown to increase with increasing particle diameter. However, there are no data available for larger liquid particles and no data for solid particles except some PSL data obtained by Cheng (1998).

The basic principle of the Aerosizer is similar to that of the TSI Aerodynamic Particle Sizer (APS). Both measure time-of-flight of particles. APS has been studied extensively (Baron *et al*., 1993). It was found that the counting efficiency of the APS nozzle is low due to impaction loss of liquid particles in the nozzle (Kinney and Pui, 1995). For solid particles, there are almost no data available for the APS, although it was indicated in a preliminary study that counting efficiency is considerably higher than that of liquid particles (Blackford *et al*., 1988). Similar impaction loss is expected to occur in the nozzle of the API Aerosizer and it is worth investigating.

To understand the particle transmission efficiency of the Aerosizer, a numerical method was developed in this study. The transmission efficiency of the nozzle is defined as the fraction of particles entering the nozzle that is detected by the laser beams downstream of the nozzle. The flow field in the nozzle was obtained from the previous study by Tsai *et al.* (1998) and the particle trajectories of both liquid and solid particles were then calculated. Effect of particle density and laser beam diameter on the transmission efficiency was also investigated. In this study, three different laser beam diameters, 300, 600 and 800 μm were assumed. The simulation for the 800 μm beam diameter is the most relevant to the performance of the API Aerosizer LD, since its nominal beam width under the nozzle is 900 μm (allowable range: 800–1000 μm). For simplicity, it is assumed that when a particle is intercepted by both laser beams, it is regarded as being detected. Scattered light intensity for a particle passing through the laser beam at different radial location is assumed to be the same. Also the transmission efficiency problems due to different settings of signal threshold and different methods of signal processing are not considered in this study.

NUMERICAL METHOD

Numerical modeling for flow field

Simulation of flow field in the nozzle and jet regime has been described in details in Tsai *et al.* (1998). The air flow in the Aerosizer is assumed inviscid, isentropic, and compressible. Two-dimensional Euler equations are converted into the non-dimensional form for the axisymmetric coordinate system as

$$\frac{\partial U}{\partial t} + \frac{\partial E}{\partial z} + \frac{\partial G}{\partial r} + H = 0, \tag{1}$$

where

$$U = \begin{bmatrix} \rho \\ \rho u \\ \rho v \\ e \end{bmatrix}, \quad E = \begin{bmatrix} \rho u \\ \rho u^2 + P \\ \rho uv \\ (e + P)u \end{bmatrix}, \quad G = \begin{bmatrix} \rho v \\ \rho uv \\ \rho v^2 + P \\ (e + P)v \end{bmatrix}, \quad H = \frac{1}{r} \begin{bmatrix} \rho v \\ \rho uv \\ \rho v^2 \\ (e + P)v \end{bmatrix}. \tag{2}$$

The unknown variables, ρ, u, v and e, in the above equations are designated the gas density, velocity components in z (axial) and r (radial) directions and total energy per unit volume, respectively. Air was assumed to behave as a perfect gas, and the pressure P is defined as

$$P = (\gamma - 1)\left[e - \frac{\rho}{2}(u^2 + v^2) \right], \tag{3}$$

where the specific heat ratio, γ, is taken as 1.4.

The total air flow rate is 5.3 l p m^{-1} with sheath flow at 3.2 l p m^{-1} and aerosol flow at 2.0 l p m^{-1}. Ambient temperature is 20°C and pressure is 1 atm. For the Aerosizer in this study, the tip of the nozzle is 750 μm in diameter and half angle is 15°. The first and second laser beams are located at 1 and 2 mm downstream of the nozzle exit, respectively.

The complete calculation algorithm and stimulation of the flow field were fully described by Tsai *et al.* (1998). The previously calculated flow field is adopted here for particle trajectory calculation.

Calculation of particle trajectory

It is assumed that the flow field is not influenced by particles with low concentrations. The calculation involves integrating particle equations of motion by means of the fourth Runge–Kutta method, applying an empirical drag law for the ultra-Stokesian regime, and neglecting the gravitational force of spherical particles. The dimensionless equations of motion of a particle in r (radial) and z (axial) directions under consideration are

$$\frac{d^2r}{dt^2} = C_d \frac{Re_p}{24} \frac{(u_r - dr/dt)}{\tau}, \tag{4}$$

$$\frac{d^2z}{dt^2} = C_d \frac{Re_P}{24} \frac{(u_z - dz/dt)}{\tau}, \tag{5}$$

where τ is the particle relaxation time defined as $\tau = \rho_p d_p^2 C/18\mu$ (ρ_p: particle density, d_p: particle diameter, C: the Cunningham slip correction factor, and μ: air dynamic viscosity), Re_p is the particle Reynolds number and C_d is the empirical drag coefficient. Also, u_r and u_z are local flow velocities in the radial and axial directions, respectively.

The dimensionless particle equations of motion are integrated through the region of interest. The initial velocity is given equal to the local flow velocity, and the initial position is set at the entrance of the nozzle. The new particle position and velocity after a small increment of time is calculated by numerical integration. The procedure is repeated until the particle passes the second laser beam.

The empirical drag coefficient, C_d, originally developed by Henderson (1976), is adopted for a wide range of flow conditions taking into account particle Mach number, M. In the subsonic flow regime, C_d is given by the following expression:

$$\begin{aligned} C_d = 24 \Bigg[Re_p + S \Bigg\{ 4.33 + \left(\frac{3.65 - 1.53\, T_w/T}{1 + 0.353\, T_w/T} \right) \exp\left(-0.247 \frac{Re_p}{S} \right) \Bigg\} \Bigg]^{-1} \\ + \exp\left(-\frac{0.5M}{\sqrt{Re_p}} \right) \left[\frac{4.5 + 0.38\,(0.03\,Re_p + 0.48\sqrt{Re_p})}{1 + 0.03\,Re_p + 0.48\sqrt{Re_p}} + 0.1M^2 + 0.2M^8 \right] \\ + \left[1 - \exp\left(-\frac{M}{Re_p} \right) \right] 0.6S. \end{aligned} \tag{6}$$

And in the supersonic regime at Mach numbers equal to or greater than 1.75, the form of C_d is

$$C_d = \frac{0.9 + (0.34/M_\infty^2) + 1.86\,(M_\infty/Re_\infty)^{1/2}\ [2 + (2/S_\infty^2) + 1.058/S_\infty\,(T_w/T)^{1/2} - 1/S_\infty^4]}{1 + 1.86\,(M_\infty/Re_\infty)}. \tag{7}$$

When the Mach number at the transition region between 1.0 and 1.75, C_d is the linear interpolation of equations (6) and (7).

In the above equations, S is the molecular speed ratio equal to $M\sqrt{\gamma/2}$; M is the particle Mach number determined by the relative velocity between the particle and air flow; T_w is

the temperature of the particle; T is the air temperature. The subscript, ∞, denotes free stream conditions.

Particles in the sampling flow would impinge on the nozzle wall when unable to follow the curving streamline near the wall because of their inertia. Solid particles that bounce back into the sampling flow may exit the nozzle, whereas liquid particles stick on the nozzle wall. When the center of a solid particle approaches the solid wall within a distance equal to its radius, the particle is considered impacted. Trajectories of rebounding particles are then simulated. The particle transmission efficiency through the nozzle is calculated by the ratio of the number of particles detected by the two laser beams to the total number of particles entering the nozzle. Only the particle that passes through both laser beams is considered to be counted.

The model developed by Xu *et al.* (1993), and Xu and Willeke (1993), which considered elastic and plastic deformation and rotation of solid particles during impact process, was adopted to calculate the rebound velocity of particles. Particle bounce may occur when its incident velocity is greater than the critical velocity. The rebound velocity and the critical velocity were found to be strongly dependent on the incident impact angle and velocity.

In this model, the kinetic energy of a impacting particle, $E_{k,i}$, is divided into normal and tangential components, $E_{k,i,n}$, and $E_{k,i,t}$. In the normal direction of impact, a particle may experience primary and secondary elastic deformations, and plastic and elastically deformed plastic deformations. In the tangential direction, only particle rotation was considered. The normal component of impact kinetic energy equals the sum of rebound, surface adhesion, elastic and plastic deformation energies as

$$E_{k,i,n} = E_{e,0} + E_{e,1} + E_{e,2} + E_p, \tag{8}$$

where $E_{e,0}$ is energy stored in primary elastic deformation, $E_{e,1}$ is energy stored in elastically deformed plastic deformation, $E_{e,2}$ is energy stored in secondary elastic deformation, and E_p is energy loss due to plastic deformation.

The rebound kinetic energy, $E_{k,r}$, is less than the impact kinetic energy because of loss of surface adhesive energies in tangential and normal directions ($E_{a,t}$ and $E_{a,n}$) and plastic energy, E_p. The relationship from energy balance is

$$E_{k,i} = E_{k,r} + E_{a,n} + E_{a,t} + E_p. \tag{9}$$

The rebound velocity is calculated from the rebound kinetic energy when the impact kinetic energy overcomes the energy loss during the impact process, as follows:

$$V_r = \sqrt{V_i^2 - \frac{2(E_{a,n} + E_{a,t} + E_p)}{m}}, \tag{10}$$

where V_i is the initial velocity and m is the particle mass.

The critical velocity, V_{cr}, is the maximum impact velocity when no rebound occurs. That is

$$V_{cr} = \sqrt{2(E_{a,n} + E_{a,t} + E_p)/m}. \tag{11}$$

Brach and Dunn (1992, 1995) have developed another bounce model. This model takes advantage of the simplicity of algebraic solutions for collisions of particles on surfaces. It applies several coefficients to describe dynamics of particle bounce. These coefficients are acquired by experimental data. After the coefficients are determined, whether particle rebound or captured can be predicted.

A kinetic coefficient of restitution, R_1, representing internal energy dissipation in the sphere is defined as

$$P_D^R = R_1 P_D^A, \tag{12}$$

where P_D^R and P_D^A are the impulses of force due to deformation of the particle in rebound (superscript "R") and approach (superscript "A") phases, respectively. The ratio of a tangential impulse component, P_t, to the corresponding normal impulse component, P_n, over approach and rebound phases is called μ_1, which is calculated as

$$P_t = \mu_1 P_n. \tag{13}$$

The ratio of the adhesion impulse, P_A^R, to the body impulse P_D^R, during rebound is called ρ_1, which is calculated as

$$P_A^R = -\rho_1 P_D^R. \tag{14}$$

Once coefficients R_1, μ_1 and ρ_1 are obtained experimentally, the particle rebound velocity is then calculated algebraically. The particle rebound velocity in the normal and tangential directions, V_n and V_t, are

$$V_n = -R_1(1 - \rho_1)\, v_n, \tag{15}$$

$$V_t = v_t - \mu_1[1 + R_1(1 - \rho_1)]v_n, \tag{16}$$

where v_n and v_t are initial normal and tangential velocities of the particle.

RESULTS AND DISCUSSION

Particle trajectoy

Particle trajectories for particle aerodynamic diameter ranging from 0.1 to 150 μm were simulated. Ambient air condition is assumed to be 20°C and 1 atm (101.33 kPa). Some typical trajectories are presented here for illustrative purposes.

Figure 1 illustrates the behavior of small 0.5 μm PSL particles. Small particles having less inertia tend to follow air streamlines. They do not impact on the wall and eventually will exit the nozzle. However, it is seen that some particles that follow the expanding jet will likely miss the laser beams. In addition, interception efficiency of small particles by laser beams is low because of their small radii. It is therefore expected that transmission efficiency of small particles is low but increases with increasing particle diameter. From light scattering point of view, smaller particles scatter less light than larger particles which may result in less counting efficiency for smaller particles. However, this effect is not considered here.

Large liquid particles will likely stick to the nozzle wall upon impact. An example of the behavior of liquid particles of 50 μm in diameter ($\rho_p = 1.05$ g cm^{-3}) is shown in Fig. 2. The

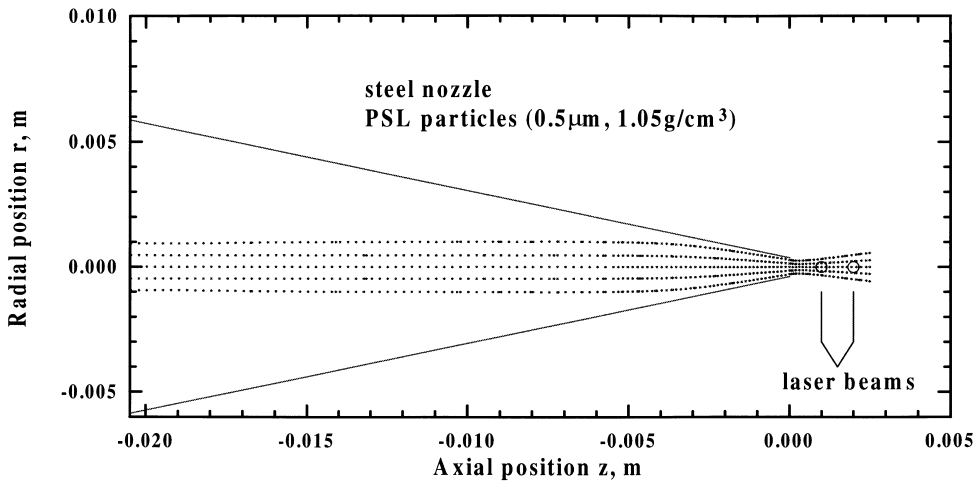

Fig. 1. Particle trajectories for PSL particles of 0.5 μm, density = 1.05 g cm^{-3}.

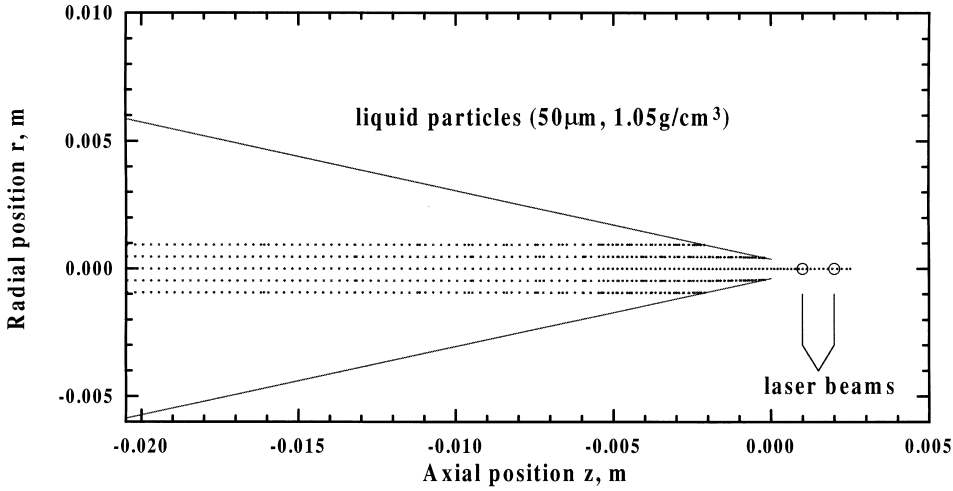

Fig. 2. Particle trajectories for liquid particles of 50 μm, density = 1.05 g cm^{-3}.

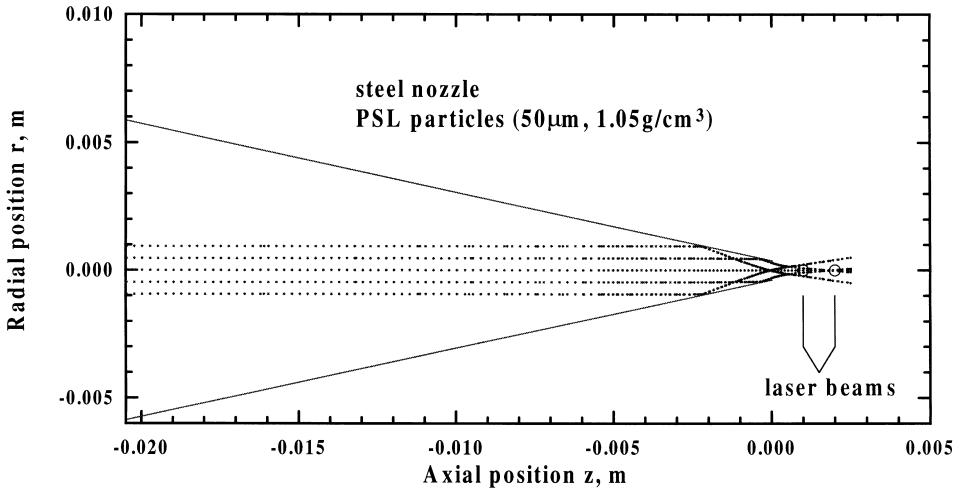

Fig. 3. Particle trajectories for PSL particles of 50 μm, density = 1.05 g cm^{-3}.

downstream laser beams cannot detect the majority of liquid particles that impact on the wall. Only a small fraction of particles near the centerline of the nozzle are likely to be detected. It is expected when impaction loss of large liquid particles becomes important, particle transmission efficiency declines with increasing particle diameter. Clogging of nozzle by large liquid particles is also expected to be severe.

In comparison, large solid particles rebound from the wall upon impact, and are likely to be detected depending on the rebound trajectory. Figure 3 shows that some large 50 μm particles may bounce into the two laser beams upon impact with the nozzle wall. Hence, its expected transmission efficiency for large solid particles is higher than that of liquid particles.

Transmission efficiency

The transmission efficiency for liquid particle (assuming $\rho_p = 1.05$ g cm^{-3}) is shown in Fig. 4. When particle aerodynamic diameter is less than 2.5, 1.7, and 0.9 μm for laser beam of 300, 600 and 800 μm in diameter, transmission efficiency increases with increasing particle diameter. This is because that larger particles do not follow expanding jet very well

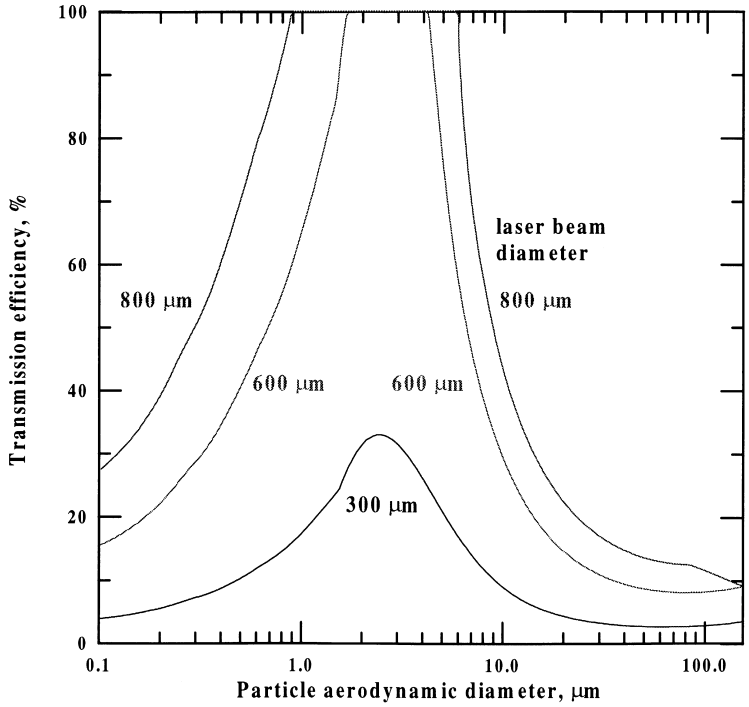

Fig. 4. Transmission efficiency for liquid particles of 1.05 g cm^{-3} in density.

and are intercepted by the laser beam more easily than smaller particles. Laser beam diameter is seen to affect particle transmission efficiency significantly. For example, when the aerodynamic diameter is 1.0 μm, transmission efficiency is 17.5, 65.6, and 99.9% for the laser beam of 300, 600 and 800 μm in diameter, respectively. Laser beam with larger diameter intercepts more particles resulting in higher transmission efficiency.

Increase in counting efficiency with increasing particle diameter was also found in the preliminary study by Cheng (1998). The unpublished data for the counting efficiency of PSL particles are: 0.594, 4.24 and 26.96% for 0.77, 0.97 and 2.76 μm particles in aerodynamic diameter, respectively.

When impaction loss occurs for particles larger than several micrometers, transmission efficiency starts to drop with increasing particle aerodynamic diameter as shown in Fig. 4. Transmission efficiency becomes less than 10% when aerodynamic diameter is greater than 100 μm. Particle density also influences transmission efficiency to a great extent due to modification of the drag coefficient caused by ultra-Stokesian motion (Tsai *et al.*, 1998) as indicated in Fig. 5 for liquid particles with density equal to 10.5 g cm^{-3}. Transmission efficiency for small particles is seen to be higher than the case of smaller particle density, 1.05 g cm^{-3}, given all other conditions fixed. Now the transmission efficiency for 1.0 μm particle is 36, 100, and 100% for the laser beam of 300, 600 and 800 μm in diameter, respectively.

While large liquid particles have low transmission efficiency, bounce of large solid particles leads to the improvement of transmission efficiency. The transmission efficiency for solid PSL particles ($\rho_p = 1.05$ g cm^{-3}) through steel nozzle is presented in Fig. 6 using the bounce model of Xu *et al.* (1993), and Xu and Willeke (1993). For small particles, impaction loss does not occur, transmission efficiency is the same as that of liquid particles. For particles larger than several micrometers in aerodynamic diameter, it is seen that now the transmission efficiency for solid particles is much higher than the case of liquid particles, Fig. 4. The improvement is more obvious when the laser beam diameter is larger. For example, when the laser beam diameter is 300 μm, particle bounce does not increase transmission efficiency until particle is greater than about 10 μm in aerodynamic diameter.

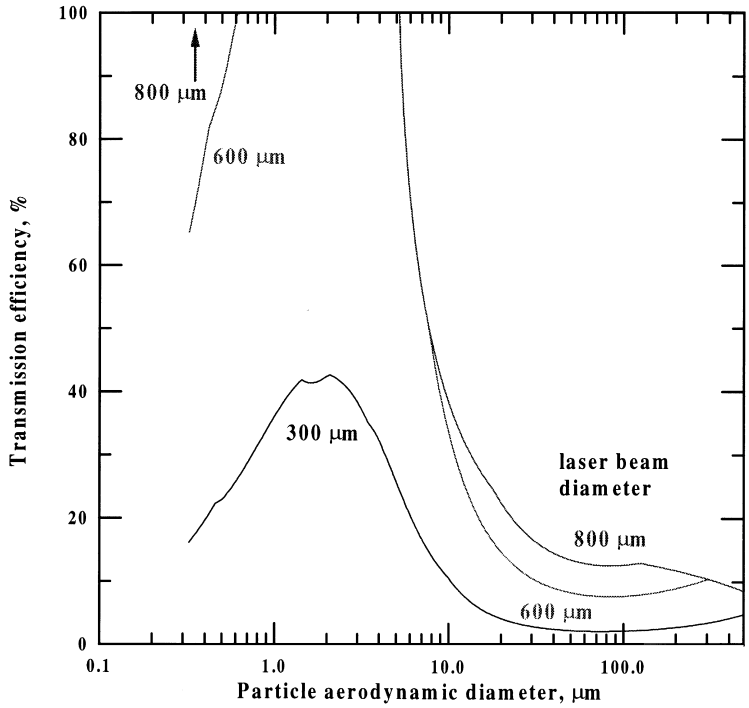

Fig. 5. Transmission efficiency for liquid particles of 10.5 g cm^{-3} in density.

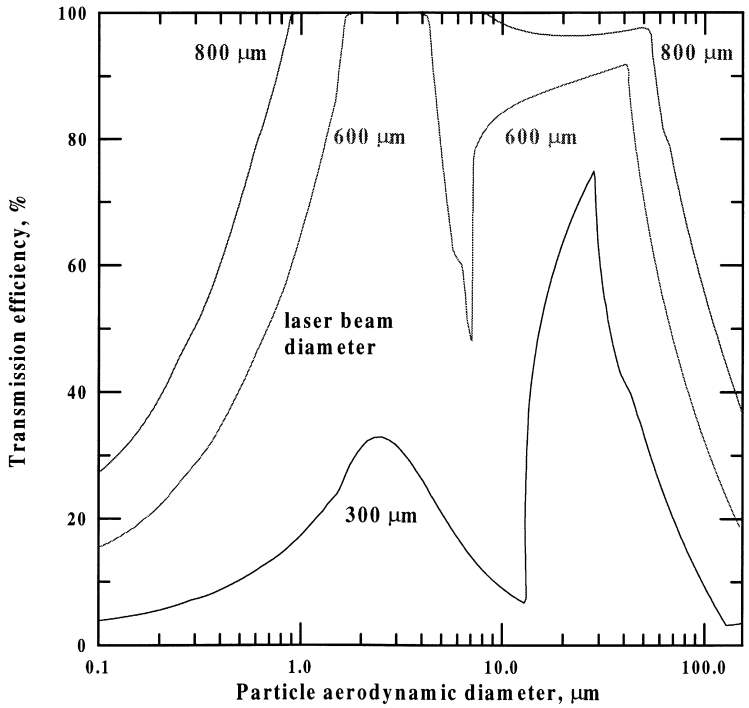

Fig. 6. Transmission efficiency for PSL particles through steel nozzle.

In contrast, for a laser beam of 800 mm in diameter, particle bounce increases the transmission efficiency dramatically. The efficiency is nearly 100% for particles of 1–70 μm in aerodynamic diameter. As particles become too large, particles acquire large enough velocity in the nozzle so that plastic deformation may occur which reduces particle rebound

velocity. In this case, transmission efficiency drops again with increasing aerodynamic diameter.

Another simulation of harder flyash particles ($\rho_p = 1.8$ g cm^{-3}) through steel nozzle was also made. It was shown that there is very little difference for the transmission efficiency compared to the case of softer PSL particles (Fig. 6) except the density effect, which increases the transmission efficiency slightly. Other material properties, such as hardness and surface energy, do not seem to influence transmission efficiency too much. Previous results were obtained using particle bounce model of Xu *et al.* (1993), and Xu and Willeke (1993). Simulations using newer bounce model of Brach and Dunn (1992, 1995) have obtained almost identical results for both PSL and flyash particles.

One advantage of the bounce model of Brach and Dunn (1992, 1995) over that of Xu *et al.* (1993) is that the former has more empirical constants for different materials than the latter. For example, for the transmission of silver-coated glass particles ($\rho_p = 2.6$ g cm^{-3}) through stainless steel nozzle, empirical constants are readily available only in the bounce model of Brach and Dunn (1992, 1995). For these materials, a separate calculation shows that the transmission efficiency curves are similar to Fig. 6 except that it remains high for particles greater 100 μm in aerodynamic diameter. This is presumably due to the difference in material properties.

CONCLUSIONS AND RECOMMENDATIONS

It is important to know the transmission efficiency versus particle aerodynamic diameter for the API Aerosizer as the instrument has been used widely to measure size distribution of aerosols. If the transmission efficiency is low or the transmission efficiency depends on particle diameter, then the interpretation of particle size distribution is difficult and may be erroneous. This study has investigated theoretically the effect of particle aerodynamic diameter, particle materials, particle density and laser beam diameter on the transmission efficiency of the API Aerosizer. In this study, it is assumed that particles exiting the nozzle and intercepted by the laser beams are detected. The transmission efficiency is calculated as the percentage of particles entering the nozzle that are detected by both two laser beams.

Small particles less than several micrometers have low transmission efficiency because laser beams intercept small particles less efficiently and particles that follow expanding jet miss the laser beams. For particles less than several micrometers, transmission efficiency increases with increasing aerodynamic diameter. When liquid particles are too large, impaction occurs to the wall of the nozzle which reduces transmission efficiency dramatically. The transmission efficiency continues to decrease with increasing aerodynamic diameter. The optimum transmission efficiency of liquid particles lies within the range from 1 to 10 μm in aerodynamic diameter when the particle density is 1.05 g cm^{-3}.

The transmission efficiency of solid particles improves a lot when particles are greater than about 10 μm because particles may rebound into the laser beams. Transmission efficiency remains the same as that of liquid particles for smaller particles which do not bounce.

Laser beam diameter has an important effect on the transmission efficiency. In this study laser beams having larger diameter are shown to provide more efficient particle detection than smaller diameter beams.

There are not enough experimental data available in the literature to validate the present theoretical study. It is recommend that careful experiments be conducted to determine the transmission efficiency of the API Aerosizer. Besides what have been treated here, many other factors that may influence the transmission efficiency of the API Aerosizer have to be considered. Finally, in view of the low transmission efficiency and its dependence on the particle properties (size, density, etc.) of the Aerosizer, improvement of the transmission efficiency of this instrument is critical and worthwhile.

Acknowledgements—The authors would like to thank the Taiwan National Science Council of the Republic of China for the financial support under Contract No. NSC 87-2211-E-009-005.

REFERENCES

API, Inc. (1992) *Aerosizer Mach 2 User Mannual Version 6.03*. API Inc., Mountain Farms Technology Park, Hadley, MA 01035, U.S.A.

Baron, P. A., Mazumder, M. K. and Cheng, Y. S. (1993) Direct-reading techniques using optical particle detection. In *Aerosol Measurement*: *Principles*, *Techniques*, *and Applications* (Edited by Willeke, K. and Baron, P. A.), p. 381. Van Nostrand Reinhold, New York.

Blackford, D. B., Hanson, A. E., Pui, D. Y. H., Kinney, P. D. and Ananth, G. P. (1988) Details of recent work towards improving the performance of the TSI aerodynamic particle sizer. *Proc. 2nd Annual Meeting of the Aerosol Society*, Bournemouth, UK, 22–44 March, 1988.

Bohan, J. F. (1996) Dry powder dispersion system for particle size analysis using aerodynamic time-of-flight. *Powder Handling Process.* **8,** 59.

Brach, R. M. and Dunn, P. F. (1992) A mathematical model of the impact and adhesion of microspheres. *Aerosol Sci. Technol.* **16,** 51.

Brach, R. M. and Dunn, P. F. (1995) Macrodynamics of microparticles. *Aerosol Sci. Technol.* **23,** 51.

Cheng, Y. S. (1998) Private communication.

Cheng, Y. S. and Dahneke, B. E. (1979) Properties of continuum source particle beams: II. Beams generated in capillary expansions. *J. Aerosol Sci.* **10,** 363.

Cheng, Y. S., Barr, E. B., Marshall, I. A. and Mitchell, J. P. (1993) Calibration and performance of an API aerosizer. *J. Aerosol Sci.* **24,** 501.

Dahneke, B. (1973) Aerosol beam spectrometry. *Nature Phys. Sci.* **244,** 54.

Dahneke, B. E. and Padliya, D. (1977) Nozzle-inlet design for aerosol beam. *Instruments in Rarefied Gas Dynamics*, **51,** Part II, p. 1163.

Dahneke, B. E. and Cheng, Y. S. (1979) Properties of continuum source particle beams. I. Calculation methods and results. *J. Aerosol Sci.* **10,** 257.

de Juan, L. and Fernandez de la Mora, J. (1997) Charge and size distributions of electrospray drops. *J. Colloid Interface Sci.* **186,** 280.

Etzler, F. M. and Deanne, R. (1997) Particle size analysis: a comparison of various methods II. *Part. Part. System Charact.* **14,** 278.

Grinshpun, S. A., Willeke, K., Ulevicius, V., Qian, Y. and Donnelly, J. (1995) Aerodynamic particle sizing of airborne bacteria. *J. Aerosol Sci.* **26,** S879.

Grinshpun, S. A., Willeke, K., Ulevicius, V., Juozaitis, A., Terzieva, S., Donnelly, J., Stelma, G. N. and Brenner, K. P. (1997) Effect of impaction, bounce and reaerosolization on the collection efficiency of impingers. *Aerosol Sci. Technol.* **26,** 326.

Henderson, C. B. (1976) Drag coefficients of spheres in continuum and rarefied flows. *AIAAJ*. **14,** 707.

Kinney, P. D. and Pui, D. Y. H. (1995) Inlet efficiency study for the TSI aerodynamic particle sizer. *Part. Part. System. Charact.* **12,** 188.

Marshall, I. A. and Mitchell, J. P. (1992) Behaviour of spheroidal particles in time-of-flight aerodynamic particle sizers. *J. Aerosol Sci.* **23,** S297.

Mitchell, J. P. and Nagel, M. W. (1996) An assessment of the API aerosizer for the real-time measurement of medical aerosols from pressurized metered-dose inhaler (pMDI) systems. *Aerosol Sci. Technol.* **25,** 411.

Qian, Y. G., Willeke, K., Ulevicius, V., Grinshpun, S. A. and Donnelly, J. (1995) Dynamic size spectrometry of airborne microorganisms—laboratory evaluation and calibration. *Atmos. Environ.* **29,** 1123.

Terzieva, S., Donnelly, J., Ulevicius, V., Grinshpun, S. A., Willeke, K., Stelma, G. N. and Brenner, K. P. (1996) Comparison of methods for detection and enumeration of airborne microorganisms collected by liquid impingement. *Appl. Environ. Microbiol.* **62,** 2264.

Thornburg, Jonathan, Cooper, S. J. and Leith, D. (1999) Counting efficiency of the API aerosizer. *J. Aerosol Sci.* **30,** 479.

Tsai, C. J., Chein, H. M., Chang, S. T. and Kuo, J. Y. (1998) Performance evaluation of an API aerosizer. *J. Aerosol Sci.* **29,** 839.

Ulevicius, V., Willeke, K., Grinshpun, S. A., Donnelly, J., Lin, X. and Mainelis, G. (1997) Aerosolization of particles from a bubbling liquid: characteristics and generator development. *Aerosol Sci. Technol.* **26,** 175.

Xu, M., Willeke, K., Biswas, P. and Pratsinis, S. E. (1993) Impaction and rebound particles at acute incident angles. *Aerosol Sci. Technol.* **18,** 143.

Xu, M. and Willeke, K. (1993) Right-angle impaction and rebound of particles. *J. Aerosol Sci.* **24,** 19.